Received: 8 November 2022 | Revised: 3 December 2022 | Accepted: 14 December 2022

DOI: 10.1002/jcla.24824

RESEARCH ARTICLE

WILEY

LIPG is a novel prognostic biomarker and correlated with immune infiltrates in lung adenocarcinoma

Shan Wang[1] | Zhaoxin Chen[1] | Hongwei Lv[1] | Cong wang[1] | Huamin Wei[2] | Jing Yu[1]

[1]Cancer Center, Beijing Friendship Hospital, Capital Medical University, Beijing, China

[2]Department of Traditional Chinese Medicine, Beijing Friendship Hospital, Capital Medical University, Beijing, China

Correspondence
Huamin Wei, Department of Traditional Chinese Medicine, Beijing Friendship Hospital, Capital Medical University, No. 95 Yong An Road, Xi Cheng District, Beijing, 100050, China.
Email: weihuamin6255@126.com

Jing Yu, Cancer Center, Beijing Friendship Hospital, Capital Medical University, No. 95 Yong An Road, Xi Cheng District, Beijing, 100050, China.
Email: yujing026@ccmu.edu.cn

Funding information
National Natural Science Foundation of China, Grant/Award Number: 81774221 and 81904102; Natural Science Foundation of Beijing Municipality, Grant/Award Number: 7212168

Abstract

Background: Although many biomarkers for lung adenocarcinoma (LUAD) have been identified, their specificity and sensitivity remain unsatisfactory. Endothelial lipase gene (*LIPG*) plays an important role in a variety of cancers, but its role in lung adenocarcinoma remains unclear.

Methods: TCGA, GEO, K-M plotter, CIBERSORT, GSEA, HPA, and GDSC were used to analyze *LIPG* in LUAD. Data analysis was mainly achieved by R 4.0.3.

Results: The expression of *LIPG* in LUAD tissues was higher than that in adjacent normal tissues, especially in women, patients aged >65 years, and those with lymph node metastasis. High expression predicted a poor prognosis. The results of enrichment analysis suggest that *LIPG* may exert profound effects on the development of LUAD through multiple stages of lipid metabolism and immune system regulation. In addition, *LIPG* expression was significantly correlated with the expression levels of multiple immune checkpoint genes and the abundance of multiple immune infiltrates, including the activated memory CD4 T cell, M1 macrophage, neutrophil, plasma cells, and T follicular helper (Tfh) cells in the LUAD microenvironment content. At the same time, patients with high *LIPG* expression respond well to a variety of antitumor drugs and have a low rate of drug resistance.

Conclusions: *LIPG* is a prognostic marker and is associated with lipid metabolism and immune infiltration in LUAD.

KEYWORDS
biomarker, immune checkpoint blocker, immune infiltrates, *LIPG*, lung adenocarcinoma

1 | INTRODUCTION

Lung cancer is a highly invasive and rapidly metastasizing type of tumor, which has been the most commonly diagnosed cancer over the course of the past decade. About 2.1 million new cases of lung cancer were confirmed in 2018, accounting for 12% of the global cancer burden.[1] From the histological perspective, lung cancer is divided into two main categories: non-small-cell lung cancer (NSCLC) and small cell lung cancer, accounting for 80% and 20% of cases, respectively. NSCLC can be further divided into three types:

Shan Wang and Zhaoxin Chen contributed equally to this work.

adenocarcinoma, squamous cell carcinoma, and large cell carcinoma. Among all pathological subtypes, the most common type is lung adenocarcinoma (LUAD), which accounts for ~40% of all lung cancer cases. These patients are already in the advanced stage of the disease when first diagnosed, and only ~25%–30% of patients can receive radical surgery.[2] Over the years, a comprehensive treatment based on surgery has failed to improve the survival rate of LUAD, where the five-year survival rate has been maintained at ~40%.[3] The search for specific tumor-predictive biomarkers that are necessary to determine the prognosis and uncover new therapeutic targets has always been a hot research subject in tumor therapy. Many biomarkers related to LUAD prognosis have been explored to date,[4–6] including carcinoembryonic antigen, programmed cell death 1 ligand 1 (PD-L1), epidermal growth factor receptor (*EGFR*), Kirsten rat sarcoma viral oncogene homolog (*KRAS*), *c-erbB2* gene, *p53* gene, Ki-67, and p185 protein. Although the above indicators can provide a prognostic value in LUAD patients or can be used as therapeutic targets, they still have some drawbacks. For example, patients with a new mutation (T790M) in exon 20 of the EGFR kinase domain (50%), cellular-mesenchymal to epithelial transition factor (c-MET) oncogene amplification (21%), or *PI3KCA* mutation developed resistance and relapsed within a short period of time.[7] Sorensen et al.[8] found no correlation between PD-L1 expression and overall survival (OS) in patients with advanced NSCLC. Therefore, finding new prognostic markers related to LUAD is of great clinical significance for improving the survival and prognosis of patients with LUAD.

Tumor cells are metabolically active and require a large number of biosynthetic precursor substances, such as ATP and lipids, to meet the energy and matrix demands needed for rapid tumor proliferation, among which lipid metabolism plays a vital role in the occurrence and development of tumors. Lipid metabolism of tumor does not only participate in tumor drug resistance[9] and metastasis[10] but also promote their genesis and development by interfering with the body's immunity.[11] A retrospective study confirmed that patients with low preoperative blood high-density lipoprotein cholesterol (HDL-C) have a poor prognosis, and HDL-C level can be an independent prognostic factor for NSCLC.[12] Existing evidence[13] has shown that inhibition of endothelial lipase (EL) can increase the level of HDL-C. EL belongs to the triacylglycerol lipase gene family, has phospholipase activity, can participate in lipoprotein metabolism, and is the key enzyme in blood HDL metabolism.[14,15] The gene encoding EL is located on human chromosome 18 (18q21.1) and is knowns as endothelial lipase gene (*LIPG*). Many previous studies have confirmed the role of *LIPG* in breast cancer,[16] gastric cancer,[17] testicular carcinoma in situ,[18] and prostate cancer.[19] However, the role of *LIPG* in LUAD has not been reported.

In the present study, bioinformatics data and clinical samples were used to verify the relationship between *LIPG* expression and survival prognosis and clinical features of LUAD. The possible roles and mechanisms of *LIPG* and its co-expressed genes in the development of LUAD were further explored.

2 | METHODS AND MATERIALS

2.1 | LUAD patient data collection

Download the gene expression profile and clinical data of the lung adenocarcinoma (LUAD) dataset from TCGA database. The mRNA data were obtained from 594 samples, including 59 normal lung tissue and 535 LUAD tissue samples. The Genomic Data Commons (GDC) data transfer tool was used to aggregate the mRNA expression data into an expression matrix, and the integration ID was converted into a gene symbol based on the annotation filling. The GEO database (http://www.ncbi.nlm.nih.gov/geo/) was systematically searched with the following keywords: "Lung adenocarcinoma" and "survival." Nine chips (GSE32863, GSE31210, GSE7670, GSE10072, GSE8894, GSE11969, GSE14814, GSE41271, and GSE42127) were selected for the final analysis. The original (.cel) and platform (GPL) files were downloaded. All matrix data were background-corrected, normalized, and log2-converted. The missing value replenishment was performed using the "affy" and "impute" packages in R software (version 4.0.3). *LIPG* gene expression data were extracted using "limma" package in R. In addition, the TCGA-LUAD dataset was analyzed using GEPIA website (http://gepia2.cancer-pku.cn/#index),[20] and several GEO datasets (GSE50081, GSE30219, GSE31210, GSE37745) were analyzed using Kaplan–Meier (K-M) plotter (https://kmplot.com/analysis/)[21]websites. Detailed inclusion information of GEO datasets is shown in Table 1.

At the same time, patients with LUAD who were pathologically diagnosed and surgically resectable in our hospital from July 2004 to June 2009 were selected as the clinical subjects of the present study. Inclusion criteria: (1) All patients were pathologically diagnosed as lung adenocarcinoma without prior or co-existing cancer; (2) all patients were diagnosed for the first time and had not received previous anticancer treatment such as radiotherapy and chemotherapy; (3) all patients received thoracoscopic radical resection

TABLE 1 Details of the lung adenocarcinoma dataset in GEO database

Dataset	Platform	Total (*N*)	Normal (*N*)	Tumor (*N*)
GSE32863	GPL6884	116	58	58
GSE31210	GPL570	246	20	226
GSE7670	GPL96	66	33	33
GSE10072	GPL96	107	49	58
GSE50081	GPL570	127	–	127
GSE30219	GPL570	85	–	85
GSE31210	GPL570	226	–	226
GSE37745	GPL570	106	–	106
GSE8894	GPL570	61	–	61
GSE11969	GPL7015	90	–	90
GSE14814	GPL96	71	–	71
GSE41271	GPL6884	183	–	183
GSE42127	GPL6884	134	–	134

of lung cancer by the same group of physicians; (4) the patient data included age, sex, clinical stage, lymph node metastasis, and distant metastasis; (5) 18–85 years old; (6) the expected survival time is more than 3 months; (7) the patient is conscious and willing to accept the examination with good compliance; and (8) ECOG 0–3. Exclusion criteria: (1) cases with incomplete medical history; (2) patients with other primary malignant tumors; (3) persons under the age of 18 or over 85 years; (4) patients with concomitant diseases associated with elevated lipid levels (such as diabetes, hyperlipidemia, or metabolic syndrome); (5) receiving hormone replacement therapy or drugs known to affect lipid metabolism; and (6) patients have poor compliance and explicitly refuse to follow visitors. Finally, a total of 142 patients with NSCLC were enrolled, including 75 males and 67 females. The age range is 20 to 84 years.

2.2 | Immunohistochemistry (IHC)

Immunohistochemical staining was performed on LUAD tissues and corresponding noncancer tissues. Paraffin-embedded tissue sections were dewaxed in xylene and dehydrated with gradient alcohol. The slices were placed in 0.3% hydrogen peroxide freshly prepared with methanol for 15 min at room temperature to inactivate endogenous peroxidase. The sections were boiled in 0.01 mol/L citronic acid buffer (pH 6.0; 95°C, 15–20 min) and cooled for antigen repair. Nonspecific binding was blocked with 10% normal goat serum blocking solution at 37°C for 30 min. The solution was then incubated with diluted primary antibody at 4°C overnight, followed by incubation with biotin-labeled secondary antibody at 37°C for 30 min. Streptomyces antimicrobial tin-peroxidase complex working solution was then added, and the sections were incubated at 37°C for 30 min. Animal serum from the same species as primary antibody or 1 × phosphate-buffered saline instead of primary antibody was used as a negative control. Tissue sections with known high expression of *LIPG* were used as positive controls. Diaminobenzidine was used to observe antibody binding. Staining was independently scored by two observers who were unaware of the clinical data. Depending on the dyeing strength, the staining intensity of 0 was labeled as -, 0.5 was labeled as +/−, 1 was labeled as +, 2 was labeled as ++, and 3 was labeled as +++. The staining intensity of 0 and 0.5 was defined as low expression, while 1, 2, and 3 were defined as high expression.

2.3 | Expression of *LIPG* gene

LIPG gene expression levels in LUAD and normal lung tissues were compared in the TCGA-LUAD and four chips (GSE10072, GSE32863, GSE31210, and GSE7670) from the GEO database, and clinical specimens were analyzed for further verification. In addition, immunohistochemical images for LUAD patients and normal lung tissue from the HPA database (https://www.proteinatlas.org/) were downloaded, and the differences between them were observed. The "limma" and "beewarm" package in R was used for analysis. The Wilcoxon test was used to compare the differences between the two groups.

2.4 | Survival analysis

The online analysis website GEPIA2 and K-M plotter were used to comprehensively analyze the relationship between *LIPG* expression and prognosis of LUAD patients in public databases, and supplement GEO datasets not mentioned in the above website. Datasets with fewer than 50 cases were excluded. Finally, TCGA-LUAD database and nine datasets (GSE50081, GSE30219, GSE31210, GSE37745, GSE8894, GSE11969, GSE14814, GSE41271, and GSE42127) in GEO database were selected and included in the present study.

2.5 | Clinical correlation analysis

TCGA-LUAD data were used to analyze the distribution of *LIPG* among gender, age, stage, and tumor node metastasis classification (TNM) stage.

In addition, the clinical data of LUAD patients were used for further validation. The clinical data of LUAD were used to analyze the correlation between the high and low expression of *LIPG* and the clinical characteristics of LUAD patients, including age, sex, pathological grade, stage, TNM stage, and distant metastasis.

2.6 | Analyzing genes co-expressed with *LIPG*

The bilateral Pearson correlation coefficient (r value) and Z-test were used to investigate the correlation between *LIPG* and other gene expression levels in TCGA-LUAD. Genes positively or negatively associated with *LIPG* was considered to be *LIPG*-related genes, also known as co-expressed genes ($|r| > 0.4$, $p < 0.001$).

2.7 | Gene oncology (GO), kyoto encyclopedia of genes and genomes (KEGG), and Gene set enrichment analysis (GSEA) enrichment analyses

LIPG and its co-expressed genes were enriched using GO and KEGG analyses. GO enrichment analysis included three aspects: biological process (BP), cellular component (CC), and molecular function (MF). BP is typically an ordered biological process with multiple steps. CC is used to describe the location of gene products in a cell. MF refers to the function of gene products. The "clusterProfiler" package in R was used for enrichment analysis. GSEA involves a calculation to identify consistent differences between two biological states and to determine the existence of statistical significance in a predefined set of genes. GSEA4.1.0 was used for GSEA, and c2.cp.kegg.v6.2 was selected as the gene

setting database. False discovery rate was considered to be significantly enriched.

2.8 | Stromal/immune score and *LIPG*

ESTIMATE, an algorithm that uses gene transcriptome data to infer stromal and immune cell infiltration in tumor tissue, was used in the present study to calculate the stromal score and immune score for LUAD.[22]

The relationship between stromal/immune score and *LIPG* expression was analyzed, and the median value was used as the dividing line of high and low score. Analysis was performed using the software packages "estimate," "survival," "survminer," and "limma" in R.

2.9 | Immune checkpoint blockade (ICB) correlation analysis

Correlations between immune checkpoint blockade (ICB) genes and *LIPG* were analyzed by using "limma," "reshape2," "ggplot2," "ggpubr," and "corrplot" packages in R.

2.10 | Evaluating the relationship between *LIPG* and immune cell infiltration (ICI) in microenvironment

CIBERSORT (http://cibersort.stanford.edu/) is a deconvolution algorithm based on gene expression that can evaluate a set of genes relative to all other gene expression changes in a sample. CIBESORT algorithm was used to predict the proportion of different ICIs in LUAD samples from the TCGA database, the difference in the number of ICIs in groups with high and low *LIPG* expression, and the correlation between *LIPG* expression and the number of ICIs.

2.11 | Drug sensitivity

The Cancer Drug Sensitivity Genomics (GDSC) Database (www.cancerRxgene.org) is a public resource for information on molecular markers of drug sensitivity and drug response in cancer cells.[23] The association between *LIPG* expression and the half-limiting dose (IC50) of antitumor drugs was investigated using GDSC database. "OncoPredict" is an R package for predicting drug sensitivity.[24] Filter condition was set to $p < 0.001$.

2.12 | Statistical analysis

The data were analyzed using R 4.0.3. The Wilcoxon test was used to compare variables between two groups, and the Kruskal–Wallis test was used to compare variables between multiple groups.

3 | RESULTS

3.1 | *LIPG* expression in LUAD tissues

First, the *LIPG* expression levels in several datasets (GSE32863, GSE31210, GSE7670, and GSE10072) in GEO database and TCGA-LUAD dataset were compared between cancer tissues from LUAD patients and normal lung tissues. Five sequences (TCGA differential analysis, TCGA-paired differential analysis, GSE32863, GSE31210, and GSE10072) showed that *LIPG* expression in LUAD tissue was significantly increased compared to that in normal lung tissue ($p = 0.003$, $p = 0.005$, $p < 0.001$, $p = 0.004$, and $p = 0.002$, respectively; Figure 1A–D,F), while other results showed no statistical significance (Figure 1E). Subsequently, IHC was used to verify the expression of *LIPG* in 142 LUAD tissues and corresponding noncancer tissues with complete clinical data, where the results showed that *LIPG* expression was located in the cytoplasm of cells (Figure 2A,B), and the expression of *LIPG* in LUAD tissues was significantly higher than that in corresponding noncancer tissues ($p < 0.001$; Figure 1G). At the same time, the IHC images of *LIPG* in LUAD and normal lung tissue samples from HPA database also showed that the staining intensity of *LIPG* in LUAD tissue samples was significantly stronger than that in normal lung tissue (Figure 2C,D).

3.2 | Relationship between *LIPG* and prognosis in LUAD patients

To investigate the relationship between *LIPG* and the prognosis of LUAD, we comprehensively searched the LUAD datasets in GEPIA and K-M Plotter websites and supplemented the datasets not mentioned in the above websites. Finally, a total of 9 public datasets were included in the analysis. Clinical data of patients with LUAD included in the present study were used to validate biogenic data. A-i in Figure 3 shows the relationship between *LIPG* and overall survival (OS) of LUAD patients. Figure 3M shows disease-free survival (DFS), and Figure 3N shows progression-free survival (PFS). Two public datasets and clinical samples showed that high *LIPG* expression was statistically associated with poor OS of LUAD ($p = 0.036$, $p = 0.021$, and $p = 0.048$, respectively; Figure 3E,G,L). Figure 3B shows the data of all LUAD datasets in K–M website, including 719 patients in total. Although the results were not statistically significant, it can be seen from the picture that LUAD patients with low *LIPG* expression showed better OS, and the two curves did not cross ($p = 0.052$). According to Figure 3A,D, patients with low *LIPG* expression showed a trend of better OS ($p = 0.38$ and $p = 0.13$). The results of the other 6 public datasets were meaningless (Figure 3C,F,H–K). In addition, we found that low *LIPG* expression suggested better DFS and PFS in LUAD patients, but the results were not statistically significant ($p = 0.38$ and $p = 0.277$; Figure 3M,N).

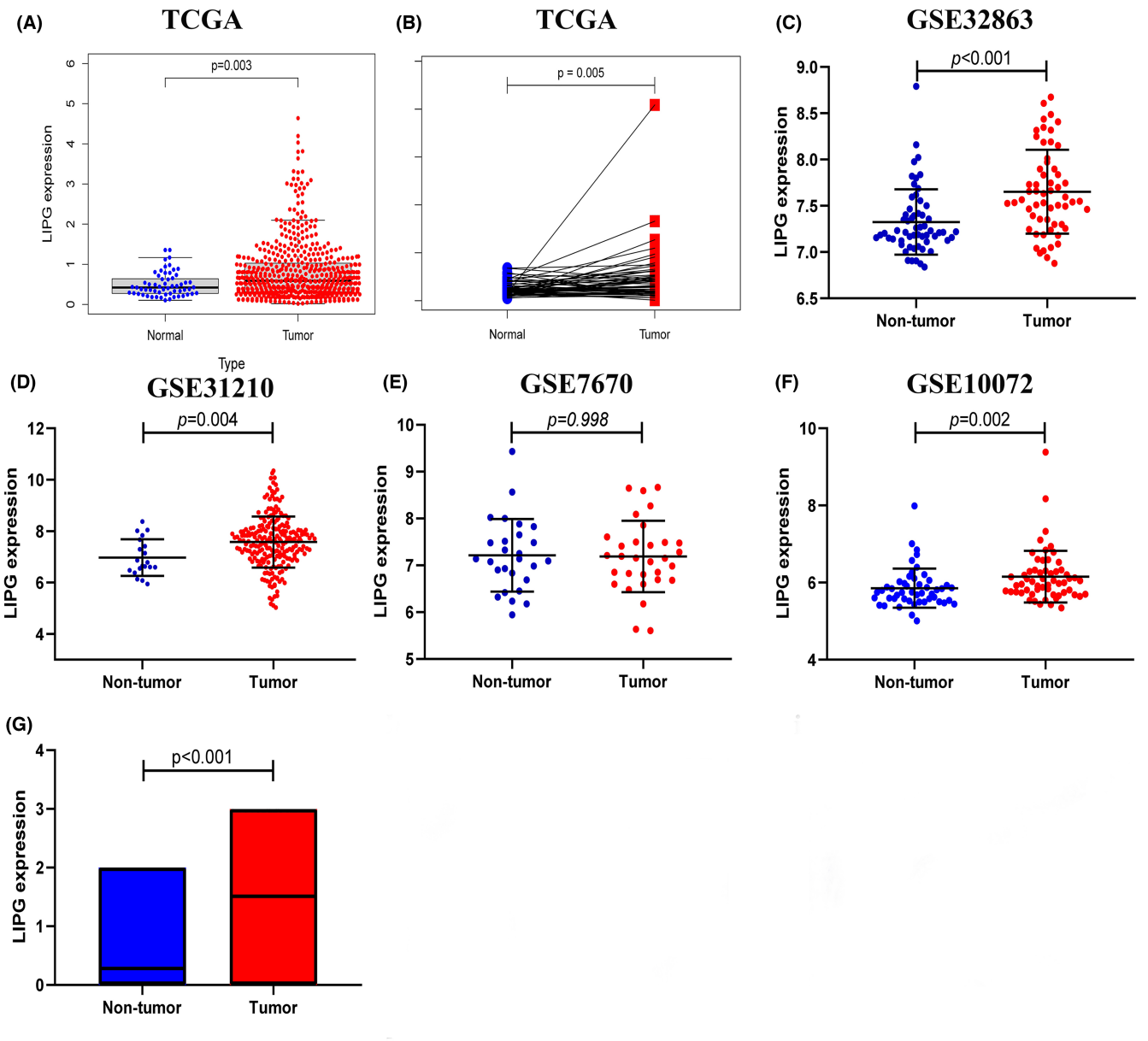

FIGURE 1 Comparison of *LIPG* expression in tumor and normal specimens. (A) Difference analysis of TCGA-LUAD. (B) Paired difference analysis of TCGA-LUAD. (C) Difference analysis of GSE32863. (D) Difference analysis of GSE31210. (E) Difference analysis of GSE7670. (F) Difference analysis of GSE10072. (G) Difference analysis of clinical samples.

3.3 | Correlation analysis between *LIPG* and clinical features

Data from the TCGA-LUAD were used to analyze the correlation between *LIPG* expression and clinical features of LUAD patients. The results showed that the age, gender, and stage of patients had a correlation with *LIPG* expression. The expression of *LIPG* was higher in women compared with men ($p = 0.0083$; Figure 4A), in LUAD patients aged >65 years compared to those <=65 years of age ($p = 0.00036$; Figure 4B), in M_0–M_1 ($p = 0.032$; Figure 4F). The distribution of *LIPG* expression in different stages was as follows: stage I > stage IV, stage II > stage IV, and stage III > stage IV ($p = 0.019$, $p = 0.012$, and $p = 0.022$, respectively; Figure 4C). However, there was no significant relationship between *LIPG* expression and T and N stages (Figure 4D,E). In addition, we divided *LIPG* expression into two groups according to the median, and the distribution of different clinical characteristics between the two groups was analyzed. Heatmap showed that the age was different between the two groups ($p < 0.001$, Figure 4G).

Subsequently, the correlation analysis of clinical samples showed that *LIPG* expression was higher in patients with lymph node metastasis ($p = 0.039$; Table 2).

3.4 | Analysis of *LIPG* co-expression genes

In order to explore the function of *LIPG*s in LUAD, microarray data of TCGA-LUAD were analyzed to identify genes co-expressed

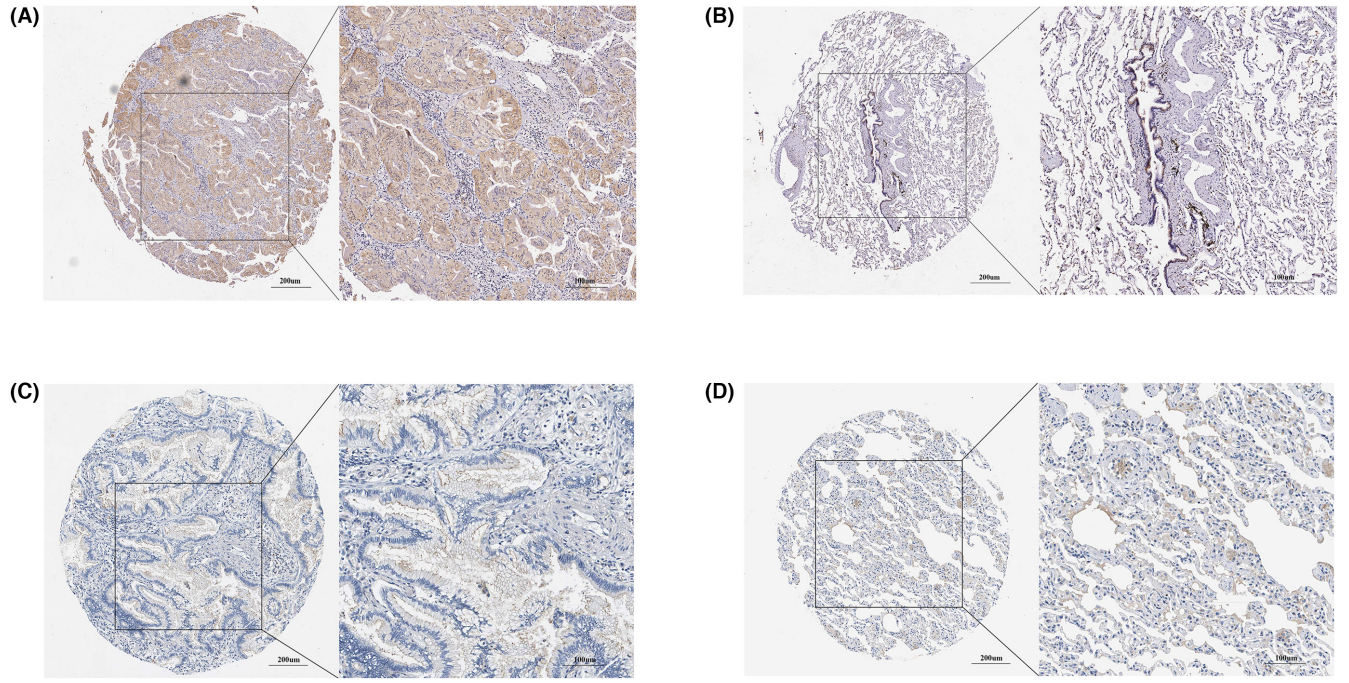

FIGURE 2 The protein expression of *LIPG* in immunohistochemical images of normal and tumor groups. (A) Immunostaining of LUAD tissues from clinical samples. (B) Immunostaining of corresponding noncancer tissues from clinical samples. (C) Immunostaining of LUAD tissues from the HPA database. (D) Immunostaining of normal lung tissues from the HPA database.

with *LIPG*. A total of 87 co-expressed genes were found. The top 8 with the strongest positive correlation with *LIPG* expression, including BICD1, ADAM19, FRMD6, and so on, were listed (Figure 5). There were no genes negatively correlated with *LIPG* expression.

3.5 | *LIPG* function in LUAD

After identifying the co-expression genes for *LIPG*, GO annotation and KEGG pathway enrichment analyses were performed. GO annotation enrichment analysis showed that *LIPG* and its co-expressed genes were mainly involved in biological processes including cell-matrix adhesion, assembly, and cell division. The gene products were located in the focal adhesion and actin, while their function included protein binding (Figure 6A,B). KEGG pathway enrichment analysis showed that *LIPG* and its co-expressed genes were involved in the focal adhesion process and Fc gamma R-mediated phagocytosis (Figure 6C,D). Pathway GSEA showed that highly expressed *LIPG*s were enriched in the Fc gamma R-mediated phagocytosis, B-cell receptor signaling pathway, natural killer cell-mediated cytotoxicity, T-cell receptor signaling pathway, and nod-like receptor signaling. Low *LIPG* expression was enriched in alpha-linolenic acid metabolism, fatty acid metabolism, arachidonic acid metabolism, linoleic acid metabolism, and steroid hormone biosynthesis pathways (Figure 6E,F).

3.6 | Stromal/immune score and *LIPG*

Through analysis, we found that compared with low expression of *LIPG*, the LUAD microenvironment with high expression of *LIPG* had more stromal cells and immune cells (Figure 7A).

3.7 | Relationship between *LIPG* expression and ICB

The role of *LIPG* in ICB treatment of LUAD has not been reported. Therefore, we used the TCGA-LUAD data to explore the correlation between *LIPG* and some ICB genes. The results showed that *LIPG* gene was positively correlated with ICB genes, including CD276, CD274, TNFRSF8, CTLA4, and so on. The correlation ranged from weak to moderate (Figure 7B).

3.8 | Relationship between *LIPG* and ICIs in LUAD microenvironment

To further explore the relationship between *LIPG* and abundance of immune infiltrates, CIBESORT algorithm was first used to predict the proportion of different ICIs in TCGA-LUAD samples. The heatmap shows 22 types of ICIs in the samples (Figure 8A), while the interrelationship between various ICIs in LUAD is represented in

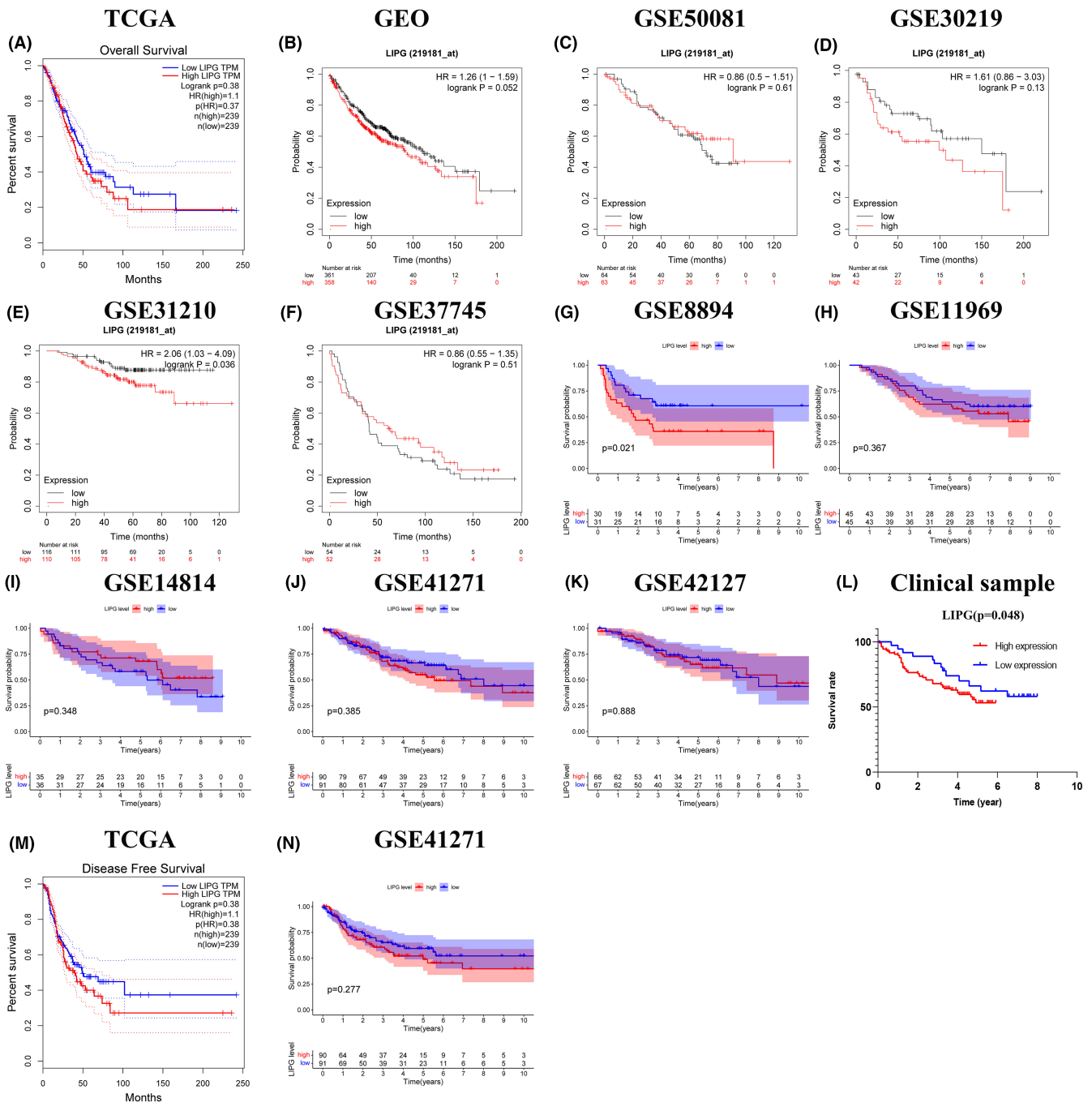

FIGURE 3 Relationship between *LIPG* gene expression and overall survival (OS), disease-free survival (DFS), and progression-free survival (PFS) in patients with LUAD. (A) Kaplan–Meier analysis of the association between *LIPG* expression and OS in TCGA-LUAD. (B) Kaplan–Meier analysis of the association between *LIPG* expression and OS in all GEO datasets of K-M Plotter. (C) Kaplan–Meier analysis of the association between *LIPG* expression and OS in GSE50081. (D) Kaplan–Meier analysis of the association between *LIPG* expression and OS in GSE30219. (E) Kaplan–Meier analysis of the association between *LIPG* expression and OS in GSE37745. (G) Kaplan–Meier analysis of the association between *LIPG* expression and OS in GSE8894. (H) Kaplan–Meier analysis of the association between *LIPG* expression and OS in GSE11969. (I) Kaplan–Meier analysis of the association between *LIPG* expression and OS in GSE14814. (J) Kaplan–Meier analysis of the association between *LIPG* expression and OS in GSE41271. (K) Kaplan–Meier analysis of the association between *LIPG* expression and OS in GSE42127. (L) Kaplan–Meier analysis of the association between *LIPG* expression and OS in clinical sample. (M) Kaplan–Meier analysis of the association between *LIPG* expression and DFS in TCGA-LUAD. (N) Kaplan–Meier analysis of the association between *LIPG* expression and PFS in GSE41271.

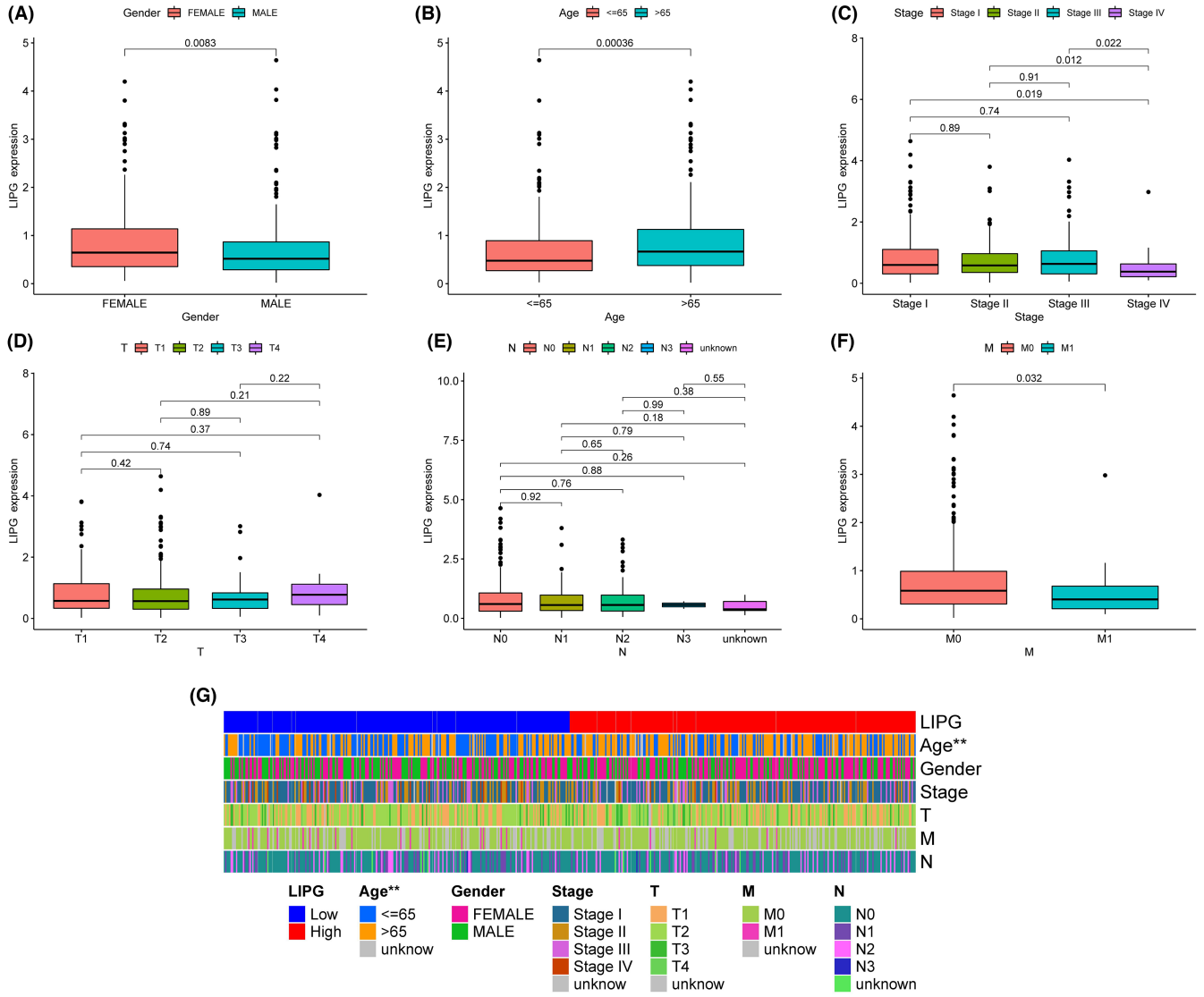

FIGURE 4 Distribution of *LIPG* expression in different clinical features in TCGA-LUAD. (A) *LIPG* expression in patients with aged ≤65 years and > 65 years. (B) *LIPG* expression in male and female patients. (C) *LIPG* expression in patients with clinical stage I, II, III, and IV. (D) *LIPG* expression in stage of T1, T2, T3, and T4 patients. (E) *LIPG* expression in stage of N0, N1, N2, and N3 patients. (F) *LIPG* expression in stage of M0 and M1 patients. (G) Heatmap shows the distribution of different clinical characteristics between high and low expression of *LIPG*.

Figure 8B. *LIPG* expression results were then divided into high and low groups in order to compare the differences in the number of ICIs (Figure 8C). The correlation between *LIPG* expression and ICI content was also analyzed (Figure 9). Finally, the result of difference and correlation analyses showed that the higher the expression level of *LIPG*, the higher the activated memory CD4 T cell, M1 macrophage, and neutrophil, and the lower the content of plasma cells and T follicular helper (Tfh) cells in the LUAD microenvironment.

3.9 | Drug sensitivity

According to the screening criteria of $p < 0.001$, a total of 16 antitumor drugs related to *LIPG* were screened. The results showed that the high expression of *LIPG* was correlated with the low IC50 value of these 16 antitumor drugs (Figure 10, Table 3), indicating that patients with high *LIPG* expression respond well to these drugs and have a low rate of drug resistance.

4 | DISCUSSION

Lipid metabolism plays a vital role in tumor treatment and development.[25–27] Therefore, looking for tumor prognostic markers associated with lipid metabolism is expected to become a new therapeutic direction. EL, as a member of the triacylglycerol lipase gene family, is a product of endothelial cells that act locally on blood vessels,[15] while the gene that encodes EL is known

TABLE 2 Relationship between *LIPG* and clinical features in human lung adenocarcinoma samples.

Clinical characters/the expression of *LIPG*	Low expression	High expression	Total(*N*)	*p*-Value
Gender				
Male	11	64	75	0.602
Female	16	51	67	
Age (year)				
<60	15	53	68	0.444
> = 60	12	59	71	
miss	0	3	3	
Pathological grade				
I	6	10	16	0.096
II	13	75	88	
III	8	29	37	
IV	0	0	0	
miss	0	1	1	
Clinical stage				
1	14	40	54	0.085
2	4	22	26	
3	4	29	33	
4	2	1	3	
miss	3	23	26	
T stage				
T1	7	34	41	0.564
T2	16	59	75	
T3	4	15	19	
T4	0	7	7	
N stage				
N0	17	53	70	0.323
N1	3	16	19	
N2	2	19	21	
N3	0	4	4	
miss	5	23	28	
Lymphatic metastasis				
Yes	17	48	65	0.039
No	9	64	73	
miss	1	3	4	
Distant metastasis				
Yes	6	16	22	0.364
No	21	91	112	
miss	0	8	8	

as *LIPG*.[28,29] Current studies have shown that *LIPG* plays a crucial part in the occurrence and development of breast cancer,[16] gastric cancer,[17] testicular carcinoma in situ,[18] and prostate cancer.[19] However, the role of *LIPG* in LUAD has not been reported. Therefore, in order to understand the biological role of *LIPG* in LUAD, bioinformatics analysis was first performed using public data and its results were validated with clinical samples to guide future studies in LUAD.

First, the analysis of multiple LUAD cohorts in the TCGA and GEO databases and clinical LUAD tissue samples revealed that *LIPG* was highly expressed in LUAD tissues compared with normal tissues. Many previous studies have explored the expression of *LIPG* in various cancer types and found it to be abnormal compared with the levels in normal tissues.[16–18] Dong et al.,[17] conducted a semiquantitative analysis of EL in urine samples from gastric cancer patients and healthy volunteers, and found that the EL content in the urine

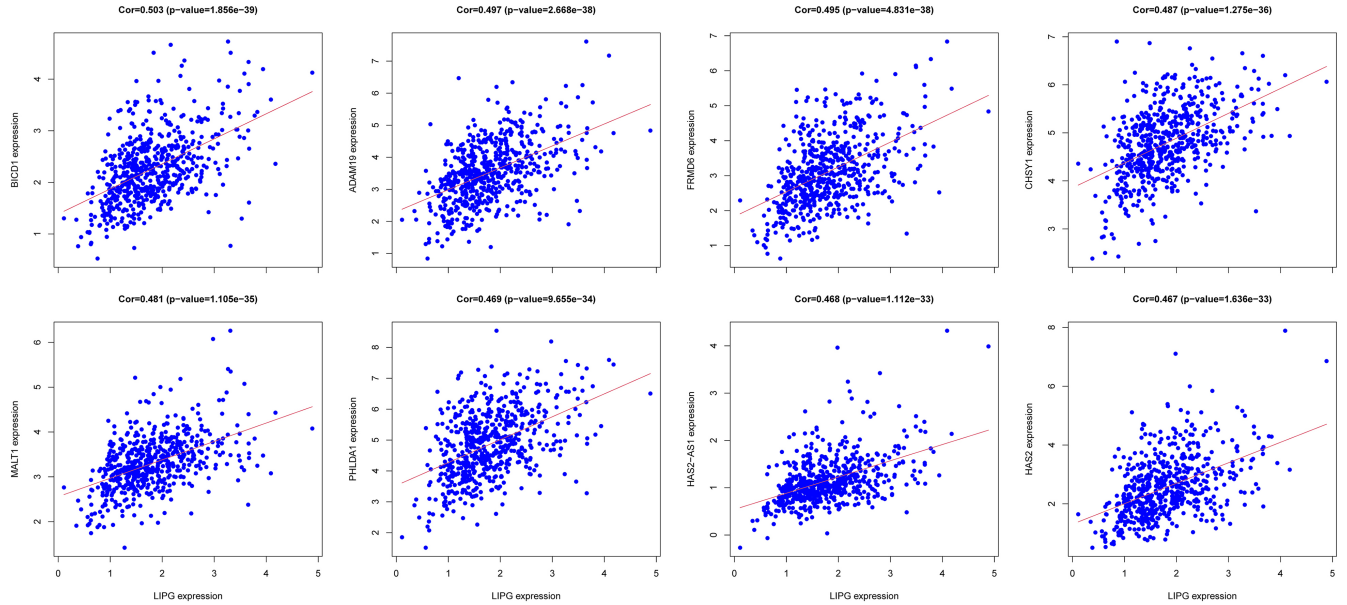

FIGURE 5 Co-expressed genes of *LIPG* in TCGA-LUAD. Genes with positive correlation with *LIPG* expression (BICD1, ADAM19, FRMD6, CHSY1, MALT1, PHLDA1, HAS2-AS1, and HAS2).

samples of healthy volunteers was about 9.9 times that of the gastric cancer patients' samples, suggesting that urinary EL level may be a highly accurate biomarker of gastric cancer. Slebe et al.[16] detected the expression of *LIPG* in 20 normal breast epithelial tissues and 20 breast cancer tissue specimens, and found that the expression of *LIPG* in breast cancer tissues was significantly higher than that in normal breast epithelial tissues, revealing the importance of *LIPG* in breast cancer. The results of this study are similar to those of previous studies. By analyzing samples from multiple sources, we found that *LIPG* expression in LUAD tissues was significantly higher than that in normal lung tissues, providing evidence for the role of *LIPG* in LUAD.

Further analysis showed that the *LIPG* expression was significantly increased in patients aged >65 years, women, and patients with lymph node metastasis ($p = 0.00036$, $p = 0.083$, and $p = 0.039$, respectively). Although the results showed that *LIPG* expression levels of stages I, II, and III patients were higher than that of IV patients, the results were of little value due to the small sample size of stage IV patients. In terms of age, we found that *LIPG* level was higher in older LUAD patients, and previous studies confirmed that the content of *LIPG* was inversely proportional to HDL-C,[13] so we speculated that the HDL-C level was lower in older LUAD patients. Many previous prospective studies have investigated the relationship between blood HDL-C level and age, and found that blood high-density lipoprotein cholesterol (HDL-C) level decreases with age,[30–34] which is consistent with our findings. Studies have shown that age can affect the reverse cholesterol transport (RCT) through factors such as insulin resistance and impaired lipolysis.[31,35] RCT has a significant impact on HDL-C levels.[31] Escolà et al.,[36] have demonstrated that the targeted inactivation of EL in mice promotes reverse cholesterol transport from macrophages to feces and enhanced the antioxidant properties of HDL. Therefore, we speculated that the high expression of *LIPG* in elderly patients may affect the RCT in LUAD patients, thereby reducing HDL-C levels. However, the specific mechanism needs to be further studied. In terms of gender, we found that *LIPG* levels in LUAD patients were higher in females than in males. The average age of both men and women in the present study was 65 years old, so we speculated that the HDL-C level of elderly women with LUAD was lower than that of men. Researches show that the average lifetime HDL-C level in women is about 10 mg/dl higher than that in men. However, HDL-C levels in men remain relatively stable with age, while HDL-C levels in women decrease with age, which may be related to changes in estrogen.[35,37] Previous studies have confirmed that the HDL-C level of postmenopausal women was significantly lower than that of premenopausal women.[38–40] The average age of both men and women in the present study was 65 years old, so we speculated that women at this age might be affected by estrogen, resulting in higher *LIPG* expression and lower HDL-C level. However, this inference still needs to be confirmed by experiments.

Survival analysis found that multiple LUAD datasets showed that high *LIPG* expression was associated with poor OS, but several datasets showed no correlation, which may be due to the small sample size. Because when we analyzed the samples of all the LUAD datasets in the K-M plotter website, we found that low *LIPG* expression showed better OS, and the two curves did not cross. In addition, we also explored the relationship between *LIPG* expression and DFS and PFS of LUAD patients, and the results showed that low *LIPG* expression showed a trend of longer DFS and PFS, but the results were not statistically significant. Previous studies have shown that LUAD patients with low preoperative blood HDL-C level have a poor prognosis. Therefore, HDL-C level can be used as a prognostic indicator for LUAD patients.[41] EL is a key enzyme in blood HDL metabolism,[14,15] and its inhibition can

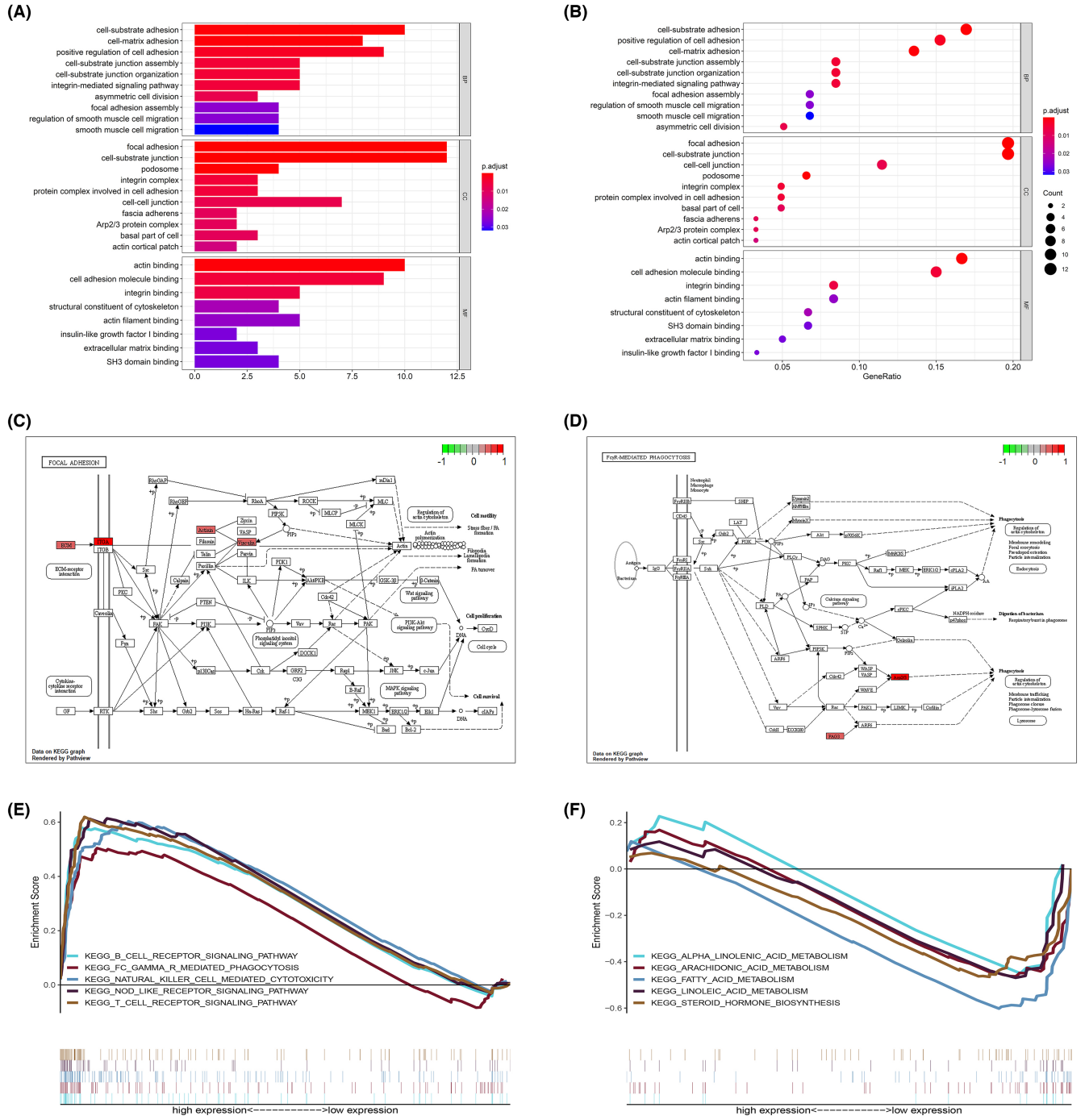

FIGURE 6 GO annotation and KEGG pathway with significant *LIPG* enrichment in LUAD. (A) The bar plot of GO annotation. (B) The bubble plot of GO annotation. (C) Path diagram of focal adhesion. (D) Path diagram of Fc gamma R-mediated phagocytosis. (E) GSEA enrichment pathway in high *LIPG* expression group. (F) GSEA enrichment pathway in low *LIPG* expression group.

improve the HDL-C level.[13] The above conclusions suggest that LUAD patients with high *LIPG* expression in cancer tissues may lead to a poor prognosis by reducing HDL levels.

In addition, a possible role of *LIPG* in the development of LUAD was explored. The role of *LIPG* in lipid metabolism and immunity was determined by identifying *LIPG* co-expression genes and using GO, KEGG, and GSEA. In terms of lipid metabolism, *LIPG* is involved in the synthesis and metabolism of lipids and may play a role in linolenic acid, arachidonic acid, fatty acid, linoleic acid metabolism, and steroid hormone biosynthesis processes. The role of *LIPG* in other types of tumors involving the lipid metabolism pathway has also been reported. Slebe et al.[42] have demonstrated that breast cancer cells rely on the lipids to provide *LIPG* for cell proliferation, while a reduction in *LIPG* expression can reduce the intracellular lipid synthesis of breast cancer cell lines MCF7 and MDA231 (glycerophospholipids, such as phosphorylethanolamine

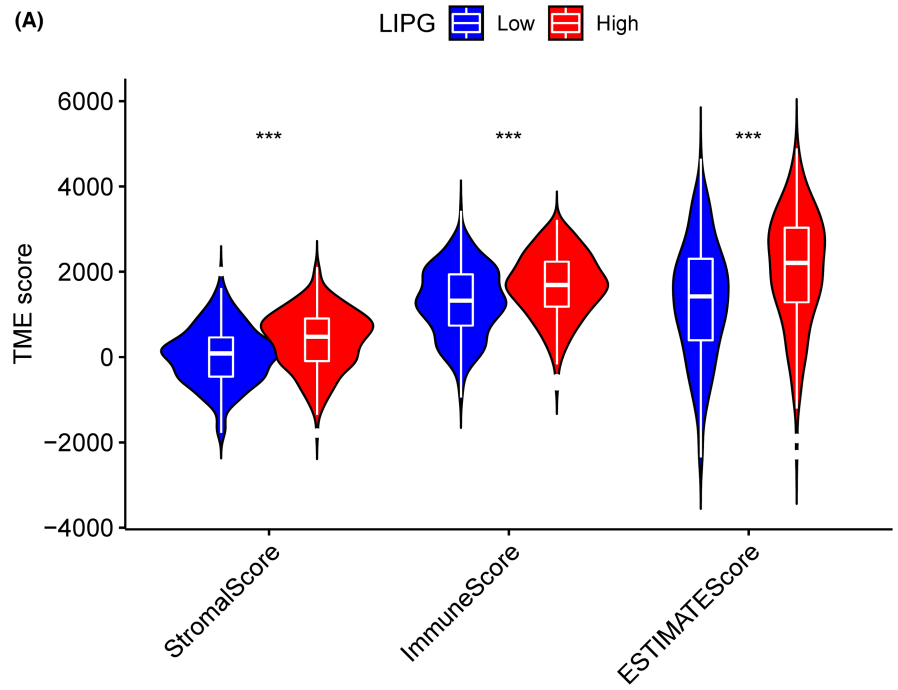

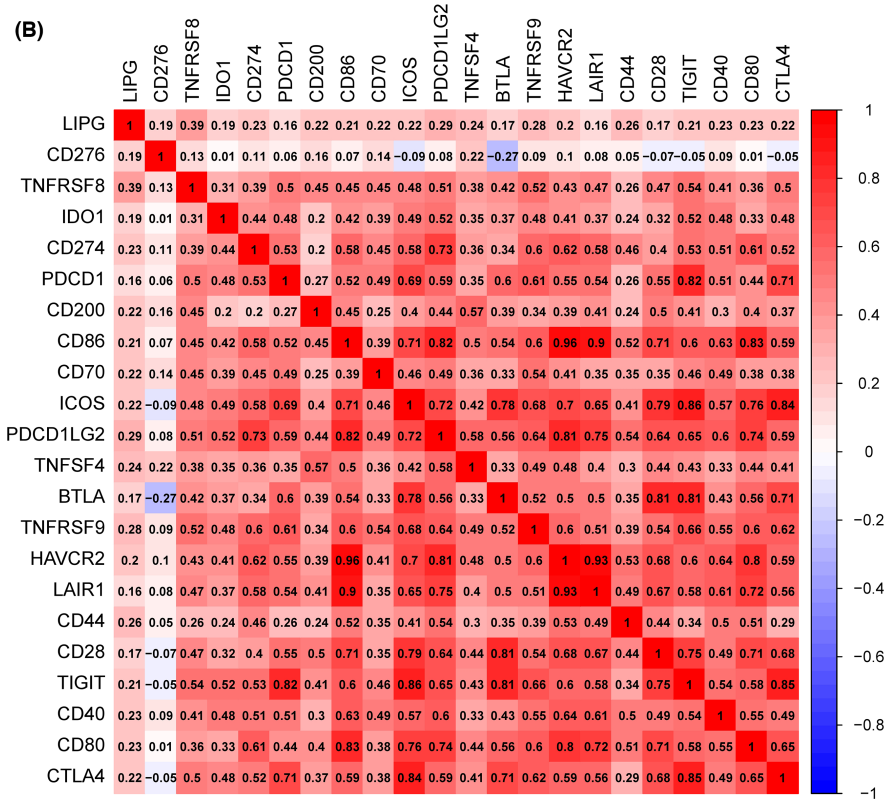

FIGURE 7 Effect of *LIPG* on immune checkpoint blockade ICB efficacy in LUAD patients. (A) Violin plot of correlation between *LIPG* expression and stromal and immune scores. (B) Heatmap of correlation between *LIPG* and ICB genes.

FIGURE 8 Difference analysis between *LIPG* and tumor-infiltration immune cells (TIICs) in LUAD microenvironment based on TCGA-LUAD. (A) Heat map of different TIICs in LUAD. (B) The interrelationship between different TIICs in LUAD. (C) Violin plot of the difference in the number of TIICs in the high and low *LIPG* expression groups. The high *LIPG* expression group has higher content of activated memory CD4 T cells, M1 macrophages, and neutrophils, while the other results showed no significant difference.

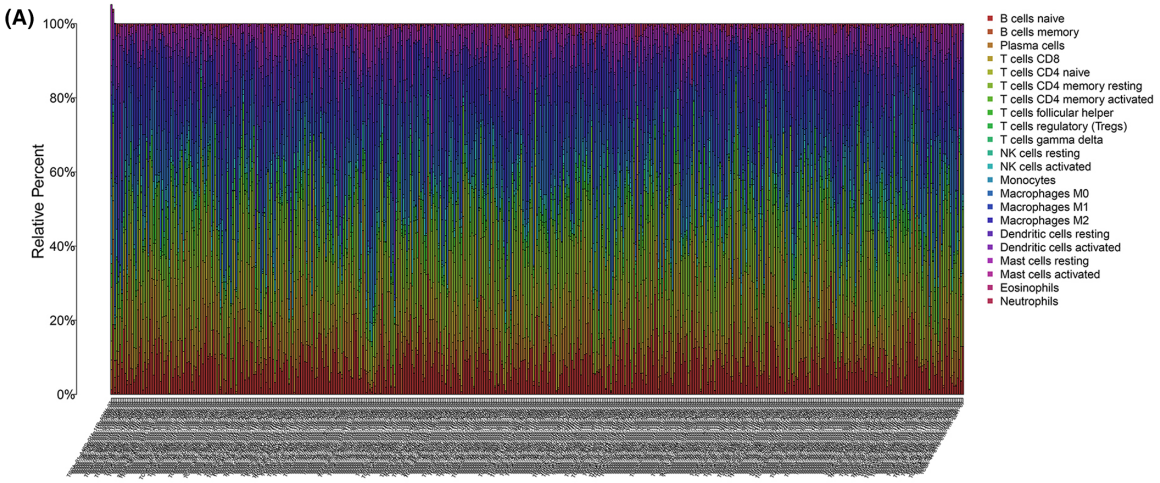
(A)
Relative Percent
100%
80%
60%
40%
20%
0%
B cells naive
B cells memory
Plasma cells
T cells CD8
T cells CD4 naive
T cells CD4 memory resting
T cells CD4 memory activated
T cells follicular helper
T cells regulatory (Tregs)
T cells gamma delta
NK cells resting
NK cells activated
Monocytes
Macrophages M0
Macrophages M1
Macrophages M2
Dendritic cells resting
Dendritic cells activated
Mast cells resting
Mast cells activated
Eosinophils
Neutrophils

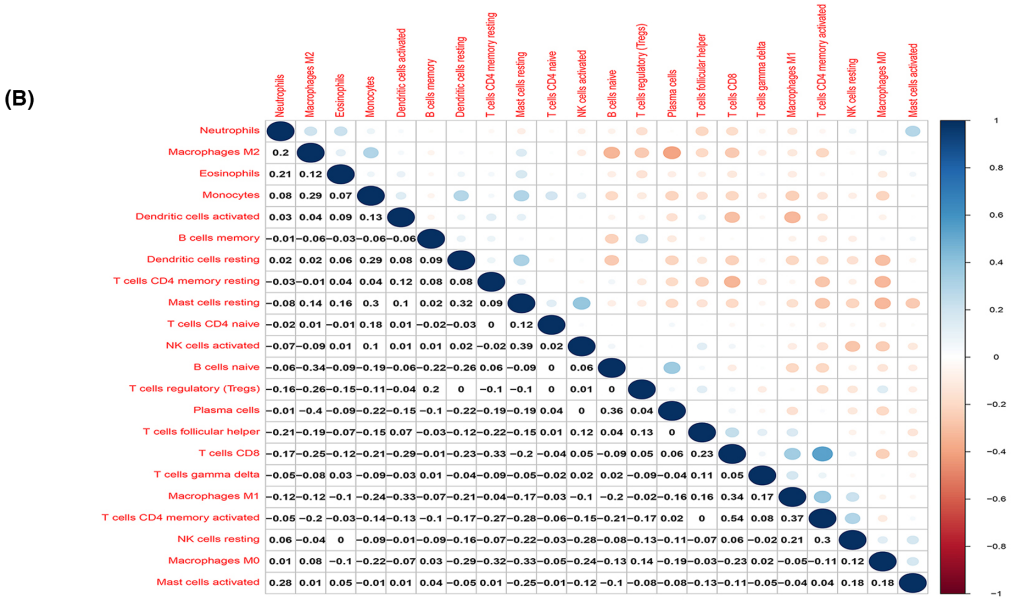
(B)
Neutrophils
Macrophages M2
Eosinophils
Monocytes
Dendritic cells activated
B cells memory
Dendritic cells resting
T cells CD4 memory resting
Mast cells resting
T cells CD4 naive
NK cells activated
B cells naive
T cells regulatory (Tregs)
Plasma cells
T cells follicular helper
T cells CD8
T cells gamma delta
Macrophages M1
T cells CD4 memory activated
NK cells resting
Macrophages M0
Mast cells activated
1
0.8
0.6
0.4
0.2
0
−0.2
−0.4
−0.6
−0.8
−1

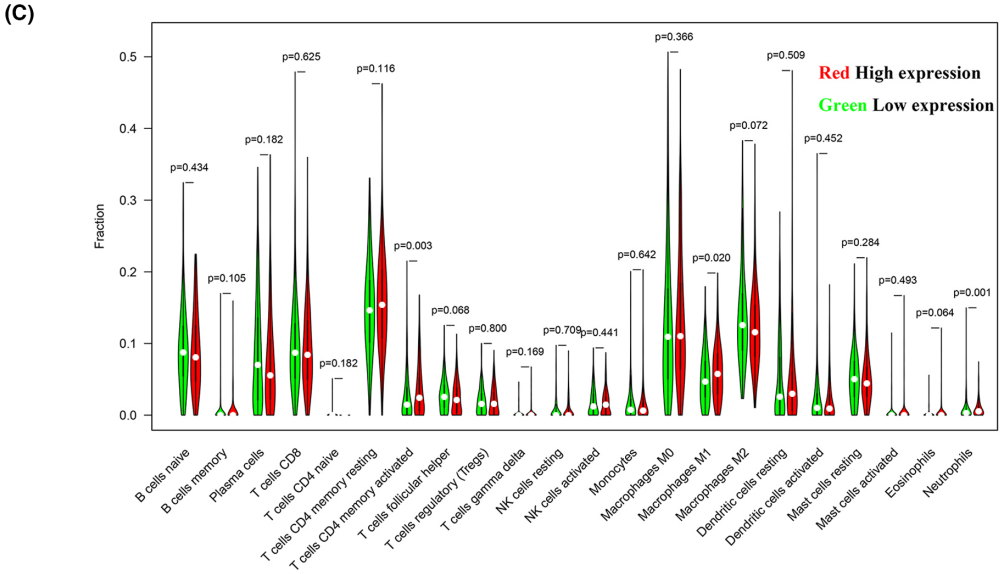
(C)
Fraction
0.5
0.4
0.3
0.2
0.1
0.0
Red High expression
Green Low expression
p=0.434
p=0.105
p=0.182
p=0.625
p=0.182
p=0.116
p=0.003
p=0.068
p=0.800
p=0.169
p=0.709
p=0.441
p=0.642
p=0.366
p=0.020
p=0.072
p=0.509
p=0.452
p=0.284
p=0.493
p=0.064
p=0.001
B cells naive
B cells memory
Plasma cells
T cells CD8
T cells CD4 naive
T cells CD4 memory resting
T cells CD4 memory activated
T cells follicular helper
T cells regulatory (Tregs)
T cells gamma delta
NK cells resting
NK cells activated
Monocytes
Macrophages M0
Macrophages M1
Macrophages M2
Dendritic cells resting
Dendritic cells activated
Mast cells resting
Mast cells activated
Eosinophils
Neutrophils

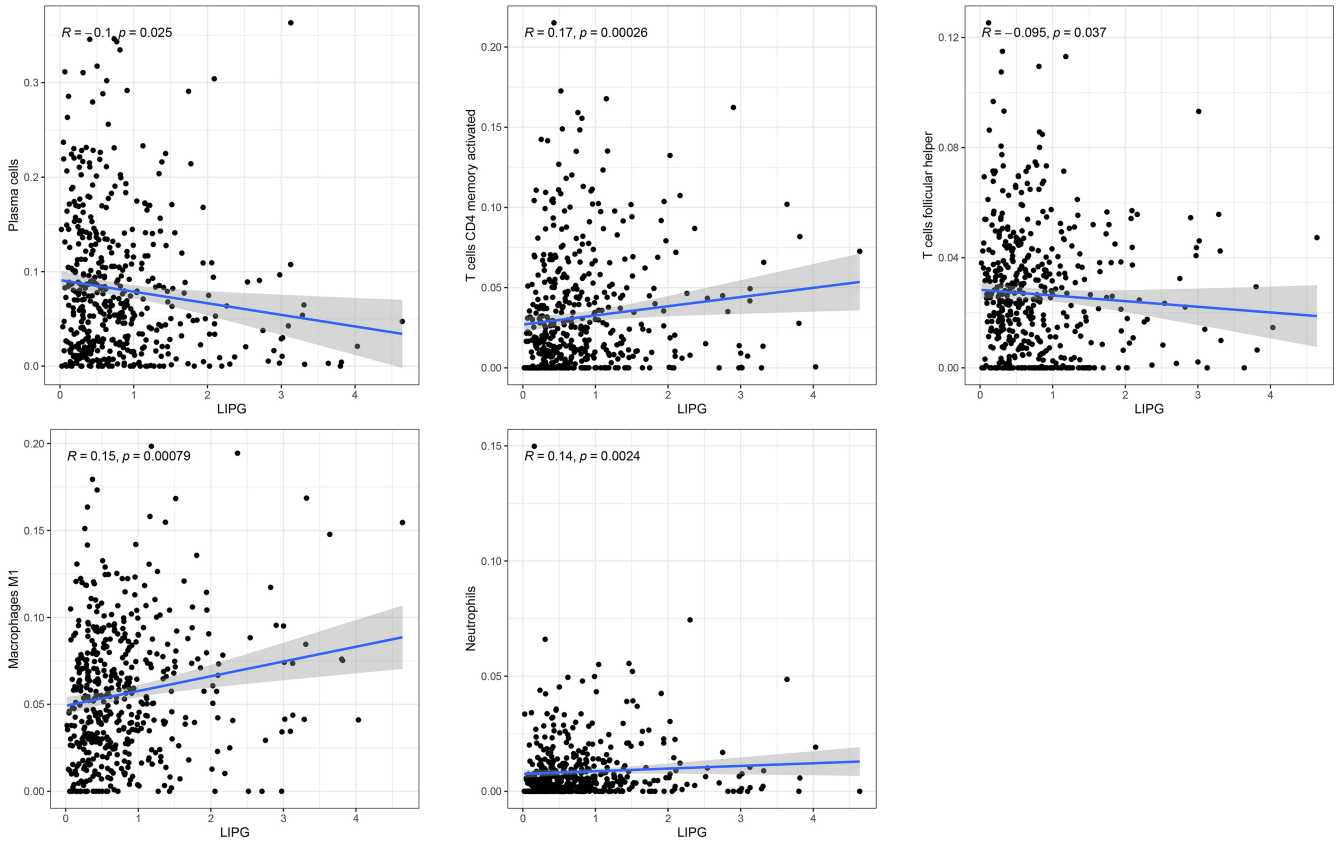

FIGURE 9 Scatter plot of correlation between *LIPG* and TIICs.

and phosphorylcholine, and glycerolipids), thereby inhibiting their proliferation. Lo et al.[16] have confirmed that *LIPG* is required for in vivo tumorigenicity and metastasis of triple-negative breast cancer (TNBC) cells. *LIPG* has a lipase-dependent function that supports cancer cell proliferation, while its lipase-independent function promotes invasiveness, stemness, and basal/epithelial–mesenchymal transition features of TNBC. Nielsen et al.,[18] have shown that *LIPG* is involved in steroidal production and nutrient supply in the testes and is important for the supply of cholesterol for testosterone production in the Leydig cells. The present study showed that *LIPG* expression in LUAD patients was significantly increased compared to that in normal lung tissue, while the high expression of *LIPG* was associated with poor OS in LUAD patients. Based on the above results, *LIPG* may be involved in lipid metabolism, cell growth, and proliferation in LUAD.

ICI therapy has great potential in cancer treatment. Previous studies have demonstrated a positive correlation between the expression of PD-L1 in tumor tissues and the response to immunotherapy.[43] However, only a subset of cancer patients can benefit from it.[44] Moreover, PD-L1 expression in a portion of patients has no correlation with OS of advanced NSCLC patients.[8] Therefore, the search for novel genes associated with ICB may provide aid for precision therapy. In the present study, we found that *LIPG* gene was positively correlated with ICB genes, including CD276, CD274, TNFRSF8, CTLA4, and so on. The influence of tumor microenvironment on the efficacy of cancer immunotherapy has attracted more and more attention. The existence of chronic inflammatory environment in lung cancer[45] may change the differentiation of immune cells and lead to the imbalance of antitumor activity, thus favoring tumor evasion[46] and developing ICB resistance.[47] Therefore, TME may be a relevant source of predictive biomarkers for ICB. Existing evidence suggests that TME performs a vital function in the determination of tumor progression and treatment outcome. As the two most important components, stromal cells, and TIICs are indispensable to the function of TME.[48–51] Through analysis, we found that compared with low expression of *LIPG*, the LUAD microenvironment with high expression of *LIPG* had more stromal cells and immune cells. Further analyses showed that the higher the expression level of *LIPG*, the higher the activated memory CD4 T cell, M1 macrophage, and neutrophil, and the lower the content of plasma cells, and Tfh cells in the LUAD microenvironment. In conclusion, we conclude that *LIPG* regulates the immune microenvironment of LUAD by interacting with macrophages, M1 macrophages, neutrophils, plasma cells, and Tfh cells, thereby influencing the efficacy of ICB. This theory needs further confirmation.

Based on the drug sensitivity analysis, we found patients with high *LIPG* expression respond well to 16 drugs and have a low rate of drug resistance, including AMG-319, AZ6102, Entospletinib, JQ1, KU-55933, MG-132, NU7441, Olaparib, PD0325901, SB216763, Selumetinib, Talazoparib, Tozasertib, Trametinib, Venetoclax, and ZM447439. However, the mechanism between *LIPG* and drug sensitivity remains to be further studied.

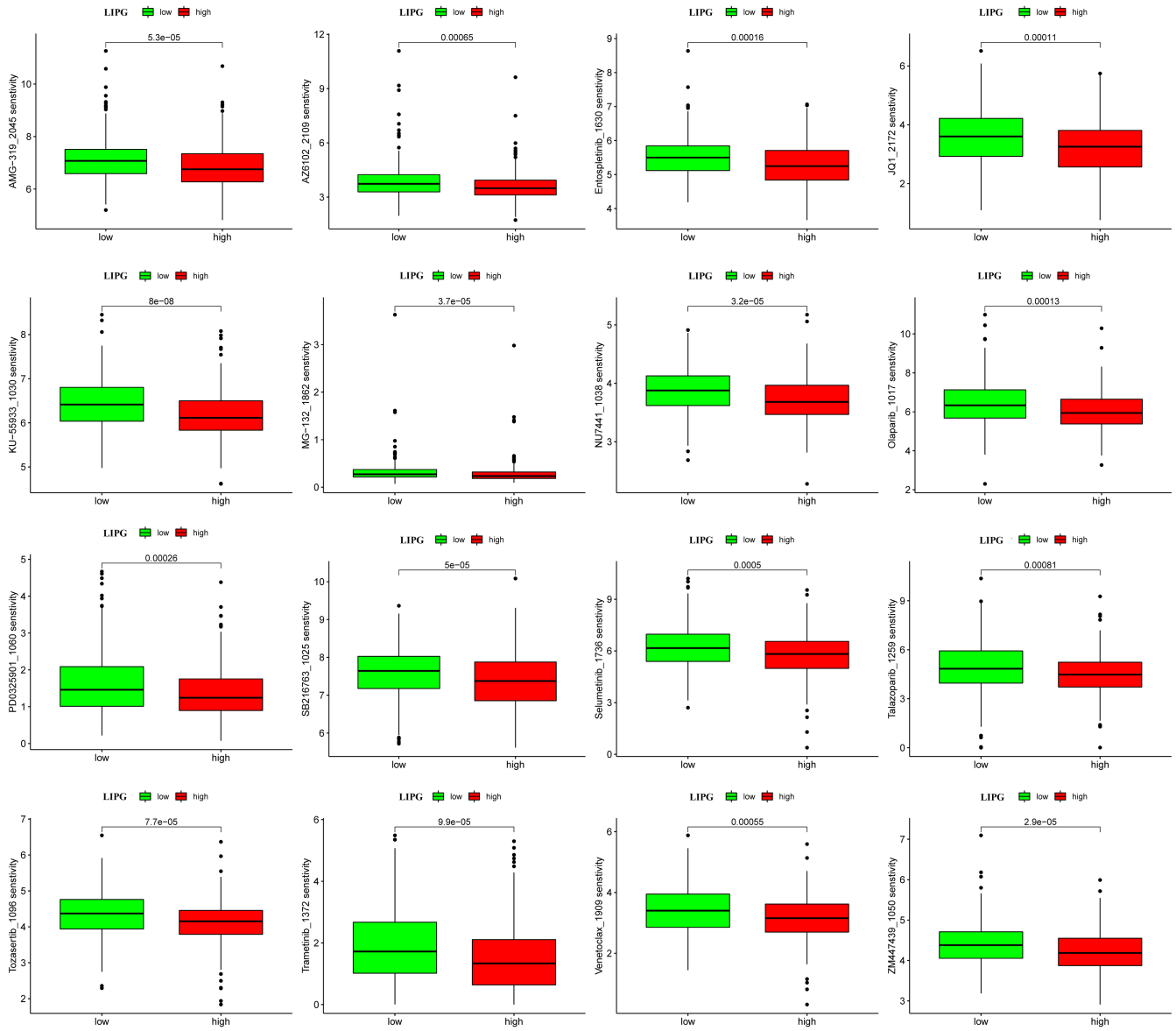

FIGURE 10 Box plot of the correlation between *LIPG* expression and the half limit dose (IC50) of antitumor drugs.

TABLE 3 Antitumor drugs associated with *LIPG*

Drug	*p*-Value
AMG-319	5.3e-05
AZ6102	0.00065
Entospletinib	0.00016
JQ1	0.00011
KU-55933	8e-08
MG-132	3.7e-05
NU7441	3.2e-05
Olaparib	0.00013
PD0325901	0.00026
SB216763	5e-05
Selumetinib	0.0005
Talazoparib	0.00081
Tozasertib	7.7e-05
Trametinib	9.9e-05
Venetoclax	0.00055
ZM447439	2.9e-05

In conclusion, the results of the present study show that *LIPG* expression is upregulated in LUAD patients, especially in women, >65 years of age, and those with lymph node metastasis. Meanwhile, high *LIPG* expression was associated with poor OS in LUAD patients. *LIPG* may also have a profound impact on the occurrence and development of LUAD via multiple stages of lipid metabolism and immune system regulation. Drug sensitivity analysis can provide individualized precision treatment for patients.

The present study provides a theoretical basis for the role of *LIPG* in the prognosis of LUAD patients, with sufficient sample size and cross-validation between bioinformatics and clinical samples increasing the credibility of the results. However, there are still some limitations in the present article. Due to COVID-19, the present study only performed pathway analysis at the bioinformatics level, lacking validation of relevant experiments. Further genomics and in vitro and in vivo studies are needed to confirm these results.

AUTHOR CONTRIBUTIONS

Wang S conducted the mining and analysis of bioinformatics data and wrote the first draft of the paper. Chen Z completed the clinical trial and conducted relevant data analysis. Lv H and Wang C participated in the auxiliary experiment and the validation of data. Yu J contributed to the project design, language polishing, and article correcting. Wei H participated in the revision of the article and the collation of some clinical data.

ACKNOWLEDGMENTS

We thank TCGA, GEO databases, GEPIA, and Kaplan–Meier (K-M) plotter for providing bioinformatics data support for the article.

FUNDING INFORMATION

This study was supported by the Beijing Natural Science Foundation of China (No. 7212168) and the National Natural Science Foundation of China (No.81774221 and No.81904102).

CONFLICT OF INTEREST

The authors declare that they have no competing interests.

DATA AVAILABILITY STATEMENT

The dataset supporting the conclusions of this article is included within the article and its supplemental tables. The datasets generated and/or analyzed during the current study are available in the Cancer Genome Atlas (TCGA, https://portal.gdc.cancer.gov/projects/TCGA-LUAD) and Gene expression omnibus (GEO, https://www.ncbi.nlm.nih.gov/gds/). The accession number is (GSE32863, GSE31210, GSE7670, GSE10072, GSE50081, GSE30219, GSE31210, GSE37745, GSE8894, GSE11969, GSE14814, GSE41271, and GSE42127, respectively). These GEO datasets can be freely and openly accessed, respectively, at https://www.ncbi.nlm.nih.gov/geo/query/acc.cgi?acc=GSE32863, https://www.ncbi.nlm.nih.gov/geo/query/acc.cgi?acc=GSE31210, https://www.ncbi.nlm.nih.gov/geo/query/acc.cgi?acc=GSE7670, https://www.ncbi.nlm.nih.gov/geo/query/acc.cgi?acc=GSE10072, https://www.ncbi.nlm.nih.gov/geo/query/acc.cgi?acc=GSE50081, https://www.ncbi.nlm.nih.gov/geo/query/acc.cgi?acc=GSE30219, https://www.ncbi.nlm.nih.gov/geo/query/acc.cgi?acc=GSE31210, https://www.ncbi.nlm.nih.gov/geo/query/acc.cgi?acc=GSE37745, https://www.ncbi.nlm.nih.gov/geo/query/acc.cgi?acc=GSE8894, https://www.ncbi.nlm.nih.gov/geo/query/acc.cgi?acc=GSE11969, https://www.ncbi.nlm.nih.gov/geo/query/acc.cgi?acc=GSE14814, https://www.ncbi.nlm.nih.gov/geo/query/acc.cgi?acc=GSE41271, and https://www.ncbi.nlm.nih.gov/geo/query/acc.cgi?acc=GSE42127.

ORCID

Jing Yu https://orcid.org/0000-0001-9521-261X

REFERENCES

1. Bray F, Ferlay J, Soerjomataram I, Siegel RL, Torre LA, Jemal A. Global cancer statistics 2018: GLOBOCAN estimates of incidence and mortality worldwide for 36 cancers in 185 countries. *CA Cancer J Clin*. 2018;68:394-424.
2. Le Chevalier T. Adjuvant chemotherapy for resectable non-small-cell lung cancer: where is it going? *Med Oncol*. 2010;21(Suppl 7):vii196-198.
3. Yao Y, Fan Y, Wu J, et al. Potential application of non-small cell lung cancer-associated autoantibodies to early cancer diagnosis. *Biochem Biophys Res Commun*. 2012;423:613-619.
4. Brower V. Biomarker studies abound for early detection of lung cancer. *J Natl Cancer Inst*. 2009;101:11-13.
5. Hilbe W, Dirnhofer S, Oberwasserlechner F, et al. Immunohistochemical typing of non-small cell lung cancer on cryostat sections: correlation with clinical parameters and prognosis. *J Clin Pathol*. 2003;56:736-741.
6. Kern JA, Robinson RA, Gazdar A, Torney L, Weiner DB. Mechanisms of p185HER2 expression in human non-small cell lung cancer cell lines. *Am J Respir Cell Mol Biol*. 1992;6:359-363.
7. Fujimoto J, Wistuba II. Current concepts on the molecular pathology of non-small cell lung carcinoma. *Semin Diagn Pathol*. 2014;31:306-313.
8. Sorensen SF, Zhou W, Dolled-Filhart M, et al. PD-L1 expression and survival among patients with advanced non-small cell lung cancer treated with chemotherapy. *Transl Oncol*. 2016;9:64-69.
9. Cao Y. Adipocyte and lipid metabolism in cancer drug resistance. *J Clin Invest*. 2019;129:3006-3017.
10. Faubert B, Solmonson A, DeBerardinis RJ. Metabolic Reprogramming and Cancer Progression. *Science*. 2020;368:eaaw5473.
11. Biswas SK. Metabolic reprogramming of immune cells in cancer progression. *Immunity*. 2015;43:435-449.
12. Chi PD, Liu W, Chen H, et al. High-density lipoprotein cholesterol is a favorable prognostic factor and negatively correlated with C-reactive protein level in non-small cell lung carcinoma. *PloS One*. 2014;9:e91080.
13. Yasuda T, Ishida T, Rader DJ. Update on the role of endothelial lipase in high-density lipoprotein metabolism, reverse cholesterol transport, and atherosclerosis. *Circ J*. 2010;74:2263-2270.
14. DeSantis P, Coleman T, Schiekofer S, Nawroth PP, Schlimmer P, Schneider JG. Endothelial lipase: a key player in HDL metabolism modulates inflammation and atherosclerotic risk. *Mini Rev Med Chem*. 2008;8:619-627.
15. Ishida T, Choi S, Kundu RK, et al. Endothelial lipase is a major determinant of HDL level. *J Clin Invest*. 2003;111:347-355.
16. Lo PK, Yao Y, Lee JS, et al. *LIPG* signaling promotes tumor initiation and metastasis of human basal-like triple-negative breast cancer. *Elife*. 2018;7:e31334.
17. Dong X, Wang G, Zhang G, et al. The endothelial lipase protein is promising urinary biomarker for diagnosis of gastric cancer. *Diagn Pathol*. 2013;8:45.
18. Nielsen JE, Lindegaard ML, Friis-Hansen L, et al. Lipoprotein lipase and endothelial lipase in human testis and in germ cell neoplasms. *Int J Androl*. 2010;33:e207-e215.
19. Riederer M, Köfeler H, Lechleitner M, Tritscher M, Frank S. Impact of endothelial lipase on cellular lipid composition. *Biochim Biophys Acta*. 2012;1821:1003-1011.
20. Tang Z, Kang B, Li C, Chen T, Zhang Z. GEPIA2: an enhanced web server for large-scale expression profiling and interactive analysis. *Nucleic Acids Res*. 2019;47:W556-w560.
21. Lánczky A, Győrffy B. Web-based survival analysis tool tailored for medical research (KMplot): development and implementation. *J Med Internet Res*. 2021;23:e27633.
22. Yoshihara K, Shahmoradgoli M, Martínez E, et al. Inferring tumour purity and stromal and immune cell admixture from expression data. *Nat Commun*. 2013;4:2612.

23. Yang W, Soares J, Greninger P, et al. Genomics of drug sensitivity in cancer (GDSC): a resource for therapeutic biomarker discovery in cancer cells. *Nucleic Acids Res*. 2013;41:D955-D961.
24. Maeser D, Gruener RF, Huang RS. Oncopredict: an R package for predicting in vivo or cancer patient drug response and biomarkers from cell line screening data. *Brief Bioinform*. 2021;22:bbab260.
25. Alavi M, Hamidi M. Passive and active targeting in cancer therapy by liposomes and lipid nanoparticles. *Drug Metab Pers Ther*. 2019;34.
26. Ogretmen B. Sphingolipid metabolism in cancer signalling and therapy. *Nat Rev Cancer*. 2018;18:33-50.
27. Pakiet A, Kobiela J, Stepnowski P, Sledzinski T, Mika A. Changes in lipids composition and metabolism in colorectal cancer: a review. *Lipids Health Dis*. 2019;18:29.
28. Jaye M, Lynch KJ, Krawiec J, et al. A novel endothelial-derived lipase that modulates HDL metabolism. *Nat Genet*. 1999;21:424-428.
29. Hirata K, Dichek HL, Cioffi JA, et al. Cloning of a unique lipase from endothelial cells extends the lipase gene family. *J Biol Chem*. 1999;274:14170-14175.
30. Cho KH, Park HJ, Kim SJ, Kim JR. Decrease in HDL-C is associated with age and household income in adults from the Korean National Health and nutrition examination survey 2017: correlation analysis of low HDL-C and poverty. *Int J Environ Res Public Health*. 2019;16:3329.
31. Walter M. Interrelationships among HDL metabolism, aging, and atherosclerosis. *Arterioscler Thromb Vasc Biol*. 2009;29:1244-1250.
32. Kreisberg RA, Kasim S. Cholesterol metabolism and aging. *Am J Med*. 1987;82:54-60.
33. Wilson PW, Anderson KM, Harris T, Kannel WB, Castelli WP. Determinants of change in total cholesterol and HDL-C with age: the Framingham study. *J Gerontol*. 1994;49:M252-M257.
34. Ferrara A, Barrett-Connor E, Shan J. Total, LDL, and HDL cholesterol decrease with age in older men and women. The Rancho Bernardo Study 1984-1994. *Circulation*. 1997;96:37-43.
35. Rohrer L, Hersberger M, von Eckardstein A. High density lipoproteins in the intersection of diabetes mellitus, inflammation and cardiovascular disease. *Curr Opin Lipidol*. 2004;15:269-278.
36. Escolà-Gil JC, Chen X, Julve J, et al. Hepatic lipase- and endothelial lipase-deficiency in mice promotes macrophage-to-feces RCT and HDL antioxidant properties. *Biochim Biophys Acta*. 2013;1831:691-697.
37. Gardner CD, Tribble DL, Young DR, Ahn D, Fortmann SP. Population frequency distributions of HDL, HDL(2), and HDL(3) cholesterol and apolipoproteins A-I and B in healthy men and women and associations with age, gender, hormonal status, and sex hormone use: the Stanford five City project. *Prev Med*. 2000;31:335-345.
38. Sultan N, Nawaz M, Sultan A, Fayaz M, Baseer A. Effect of menopause on serum HDL-cholesterol level. *J Ayub Med Coll Abbottabad*. 2003;15:24-26.
39. Reddy Kilim S, Chandala SR. A comparative study of lipid profile and oestradiol in pre- and post-menopausal women. *J Clin Diagn Res*. 2013;7:1596-1598.
40. Krauss RM, Lindgren FT, Wingerd J, Bradley DD, Ramcharan S. Effects of estrogens and progestins on high density lipoproteins. *Lipids*. 1979;14:113-118.
41. Aftergut K, Curry M, Cohen J. Candida antigen in the treatment of basal cell carcinoma. *Dermatologic Surg*. 2005;31:16-18.
42. Slebe F, Rojo F, Vinaixa M, et al. FoxA and *LIPG* endothelial lipase control the uptake of extracellular lipids for breast cancer growth. *Nat Commun*. 2016;7:11199.
43. Frelaut M, Le Tourneau C, Borcoman E. Hyperprogression under immunotherapy. *Int J Mol Sci*. 2019;20:2674.
44. Gulley JL, Rajan A, Spigel DR, et al. Avelumab for patients with previously treated metastatic or recurrent non-small-cell lung cancer (JAVELIN solid tumor): dose-expansion cohort of a multicentre, open-label, phase 1b trial. *Lancet Oncol*. 2017;18:599-610.
45. Tan Z, Xue H, Sun Y, Zhang C, Song Y, Qi Y. The role of tumor inflammatory microenvironment in lung cancer. *Front Pharmacol*. 2021;12:688625.
46. Murciano-Goroff YR, Warner AB, Wolchok JD. The future of cancer immunotherapy: microenvironment-targeting combinations. *Cell Res*. 2020;30:507-519.
47. O'Donnell JS, Teng MWL, Smyth MJ. Cancer immunoediting and resistance to T cell-based immunotherapy. *Nat Rev Clin Oncol*. 2019;16:151-167.
48. Lin WW, Karin M. A cytokine-mediated link between innate immunity, inflammation, and cancer. *J Clin Invest*. 2007;117:1175-1183.
49. Kalluri R, Zeisberg M. Fibroblasts in cancer. *Nat Rev Cancer*. 2006;6:392-401.
50. Räsänen K, Vaheri A. Activation of fibroblasts in cancer stroma. *Exp Cell Res*. 2010;316:2713-2722.
51. De Wever O, Demetter P, Mareel M, Bracke M. Stromal myofibroblasts are drivers of invasive cancer growth. *Int J Cancer*. 2008;123:2229-2238.

How to cite this article: Wang S, Chen Z, Lv H, wang C, Wei H, Yu J. *LIPG* is a novel prognostic biomarker and correlated with immune infiltrates in lung adenocarcinoma. *J Clin Lab Anal*. 2023;37:e24824. doi:10.1002/jcla.24824